

## DNS of Flow and Heat Transfer Characteristics of Multiple Impinging Jets

T SUZUKI<sup>1</sup>, K TSUJIMOTO<sup>1</sup>, T SHAKOUCHI<sup>1</sup> and T ANDO<sup>1</sup>

<sup>1</sup>Division of Mechanical Engineering, Graduate school of Engineering  
 Mie University, Kurimamachiya-cho 1577, Tsu, Mie, 514-8507 Japan

### Abstract

Multiple impinging jet (MIJ) is widely used for cooling of industrial applications such as electric device, blades of gas turbine, hot steel and so on, since it possesses high performance of heat transfer rate and is easier to implement into various systems. Thus, in order to improve the heat transfer performance, it is indispensable to elucidate the detail of flow phenomenon. In the present study, in order to analyze the flow and heat transfer characteristics formed by the interaction of MIJ, we conduct the DNS (direct numerical simulation) of 13 and 19 round impinging jets and investigate the influence of interference between jets. From the instantaneous velocity distribution, it is observed that each jet impinges the impingement wall and diffuses in the radial direction in both multiple jets. From the time-averaged velocity and Nusselt number distribution, it is confirmed that flow phenomena such as up-wash flow due to the interaction between jets are generated and that the Nusselt number shows a high value at the impinging points and decreases toward the outside of the calculation region. In addition the heat transfer performance decreases in the interaction region between the jets.

### Introduction

Impinging jet is widely used for cooling of industrial applications such as electric device, blades of gas turbine, hot steel and so on, since it possesses high performance of heat transfer rate and is easier to implement into various system. Their characteristics are reviewed by a few notable literatures[7, 14]. Impinging jets are subdivided into three regions, such as free jet region, stagnation region and wall jet region[14]. Their performance of heat transfer on the impingement wall is depending on the Reynolds number, the shape of nozzle, the number of nozzle, the distance between the nozzle and the impingement wall and so on[14]. In particular, although a single impinging jet produces high heat transfer rate around an impinging position on an impingement wall, the heat transfer performance decays with increasing the distance from the impinging position. Thus in order to overcome the shortcoming of single impinging jet (SIJ), i.e., the occurrence of both inhomogeneous heat distribution on the wall and the narrow heating area, MIJ is generally introduced in industrial applications. Thus far it is well-known that each jet of MIJ interacts with each other, producing a complex flow field[4, 15]. In addition, the heat transfer performance is significantly influenced with their interaction. Therefore to realize an optimum heat transfer performance, the influence of geometrical arrangement of jets, i.e., the separation length between jets, the arrangement pattern, should be investigated. Recently significant advances of computer power lead to the realization of fluid phenomena including miniature vortices through the DNS. Under the state of the art, we found the effectiveness of the active control of a round jet for the mixing enhancement[13]. Also DNS of impinging jets and highly resolved LES (large eddy simulation)[5] have demonstrated the flow structure and the statistical properties of heat transfer. Hence at present computer simulations are capable of conducted so far [5, 6, 12] systematically investigating the effect of control parameter. The

computer simulation of SIJ using RANS, LES, and DNS has already been conducted, however, since for the MIJ it needs a huge computer power, steady flow simulations are mainly conducted. In addition, since there is no reliable turbulence model for multiple impinging jets, low Reynolds number flows (laminar flows) of MIJ are mainly investigated[1]. Recently the LES of MIJ just appeared[3, 9], however, the results of thermal field were not well reported. In the present study, we conduct DNS of 13 and 19 round impinging jets and investigate the influence of interference between jets.

### Numerical method

#### Governing equations and their discretization

Under the assumption of incompressible flow, the governing equations are as follows:

$$\frac{\partial u_i}{\partial x_i} = 0 \quad (1)$$

$$\frac{\partial u_i}{\partial t} + h_i = -\frac{\partial p}{\partial x_i} + \frac{1}{Re} \frac{\partial^2 u_i}{\partial x_j \partial x_j} \quad (2)$$

( $h_i = \varepsilon_{ijk} \omega_j u_k$ ,  $\omega_j$ : vorticity)

$$\frac{\partial T}{\partial t} + u_i \frac{\partial T}{\partial x_i} = \frac{1}{RePr} \frac{\partial^2 T}{\partial x_j \partial x_j} \quad (3)$$

where  $u_i$  is velocity component,  $p$  is total pressure,  $T$  is temperature and  $\varepsilon_{ijk}$  is Levi-Civita symbol. The convective terms of Eq.(2) is described as rotational form. Above equations are normalized by both the diameter of the inlet jet,  $D$  and the inlet velocity,  $V_0$ . Reynolds number and Prandtl number are defined as  $Re = V_0 D / \nu$  ( $\nu$ : dynamic viscosity) and  $Pr = \nu / \alpha$  ( $\alpha$ : thermal conductivity), respectively. The computational volume is a rectangular box. The origin of axes is set at the center of an impingement wall. The wall-normal direction,  $y(=x_2)$  and two horizontal directions,  $x(=x_1)$ ,  $z(=x_3)$  are set, and the velocity component for each direction denotes  $u(=u_1)$ ,  $v(=u_2)$  and  $w(=u_3)$ , respectively. The spatial discretization is performed with sine or cosine series expansion in  $x$  and  $z$  directions and 6th-order compact scheme[8] in  $y$  direction. The velocity components are discretized as follows so that the boundary conditions are satisfied:

$$\begin{aligned} u(x, y, z) &= \sum u_{mn}(y) \cos(k_m x) \sin(k_n z) \\ v(x, y, z) &= \sum v_{mn}(y) \sin(k_m x) \sin(k_n z) \\ w(x, y, z) &= \sum w_{mn}(y) \sin(k_m x) \cos(k_n z) \end{aligned} \quad (4)$$

In order to remove the numerical instability due to the nonlinear terms, the 2/3-rule[2] is applied for the horizontal directions and an implicit filtering for the wall-normal direction is conducted with 6th order compact scheme. For the time advancement, third order Adams-Bashforth method is used. The well-known MAC method is employed for pressure-velocity coupling, which results in a Poisson equation for the pressure. After the Poisson equation is expanded with sine series in  $x$  and  $z$  directions, the independent differential equations are obtained for each wave number and then is discretized with sixth order com-

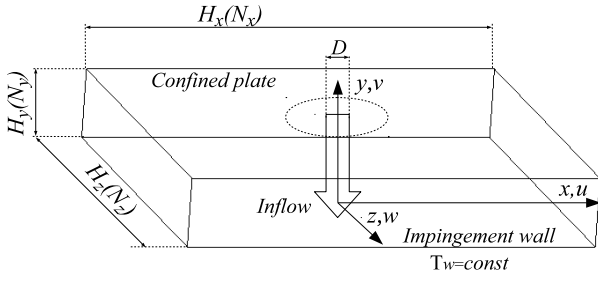


Figure 1: Coordinate system and computational domain

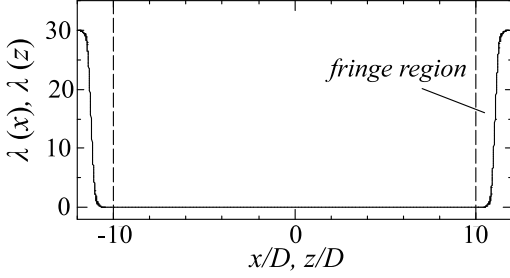


Figure 2: Sample fringe function

compact scheme. Finally, the penta-diagonal matrix is deduced for each wave number. In the present simulation code, these matrices are solved using the LU Decomposition method. When vortical structures approach the side boundary of impingement wall, relatively strong low-pressure regions being formed by vortical structures do not meet the pressure boundary condition, *i.e.*  $p = 0$ . In the present simulation, since the spectral method is used, the occurrence of this discrepancy at the side boundary induces the unphysical numerical oscillation in the whole flow field. Thus the vortical motions should be artificially reduced near the boundary. In the present simulation, a fringe (buffer) region[10] is introduced around side boundary in order to reduce the perturbation using an appropriate external force. The external force is assumed to be as follows:

$$G = -\lambda(u - u_{ref})$$

where  $u_{ref}$  is objective velocity. Thus the external force continues to work until the objective velocity is attained. In the present simulation, in order to allow smooth flow outside the computational domain, the external force normal to the side boundary is set to zero, while the tangential component of external force is imposed under the condition  $u_{ref} = 0$ . Finally the external forces are determined as follows:

$$\begin{aligned} G_x &= -\lambda(z)u \\ G_y &= -(\lambda(x) + \lambda(z))v \\ G_z &= -\lambda(x)w \end{aligned} \quad (5)$$

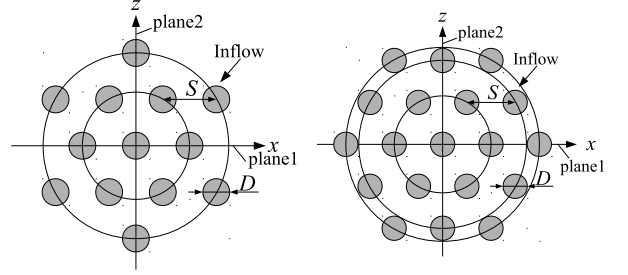
where the coefficient  $\lambda$  means strength of the external force. In the present computations,  $\lambda$  is set as shown in figure 2.

#### Calculation conditions

The inlet velocity distribution is assumed to be top-hat type, which is given as follows:

$$V_{in}(r) = \frac{V_0}{2} - \frac{V_0}{2} \tanh \left[ \frac{1}{4} \frac{R}{\theta_0} \left( \frac{r}{R} - \frac{R}{r} \right) \right] \quad (6)$$

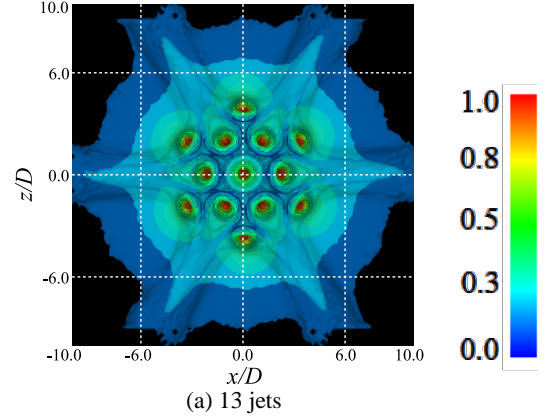
where  $V_0$  is the center velocity,  $\theta_0$  denotes the initial momentum thickness and  $R (= D/2)$  is radius of an inlet jet. This inlet velocity profile is selected by referring to the literature[11].



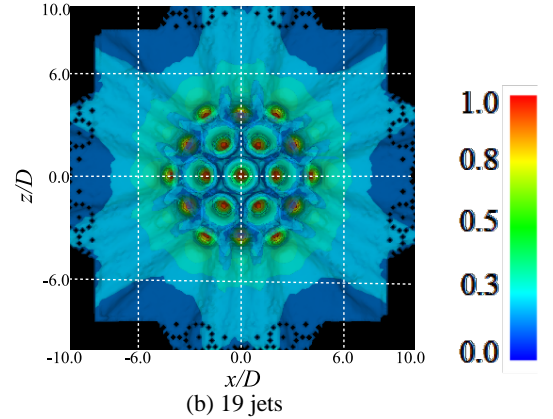
(a) 13 jets

(b) 19 jets

Figure 3: Geometrical arrangements of nozzles



(a) 13 jets



(b) 19 jets

Figure 4: Contour of mean velocity magnitude

( $R/\theta_0 = 20$ ). In the present simulations, the distance to the impingement wall,  $H$  is  $H/D = 4$ . Computational conditions such as the size of computational domain, the grid number, the Reynolds number, the Prandtl number is  $(H_x, H_y, H_z) = (24D, 4D, 24D)$ ,  $(N_x, N_y, N_z) = (128, 100, 128)$ ,  $Re = 1500$  and  $Pr = 0.71$ , respectively. The grid spacing of wall-normal direction is densely populated near wall region. The inflow temperature,  $T_0$  and the ambient temperature,  $T_a$  are assumed to be higher than the wall temperature,  $T_w$ , *i.e.*,  $T_0 = T_a > T_w$ . The statistical properties are averaged over the time. In the present study, with reference to the paper[9] 13 and 19 jets are arranged as shown in figure 3. The separation between jets  $S$  is  $S/D = 2.0$

## Results and discussions

### Flow structure

The 3D contour surfaces of time-averaged velocity magnitude observed from the inlet of jets are shown in figure 4. It is observed that from each inlet which is colored red in figure 4,

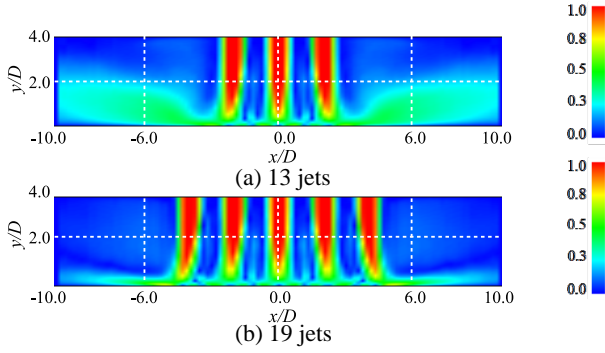


Figure 5: Contour of mean velocity magnitude on plane1

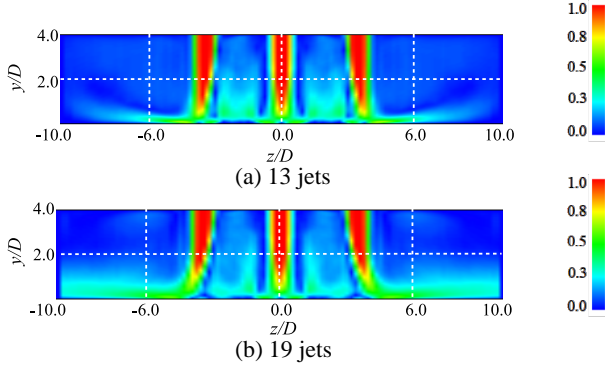


Figure 6: Contour of mean velocity magnitude on plane2

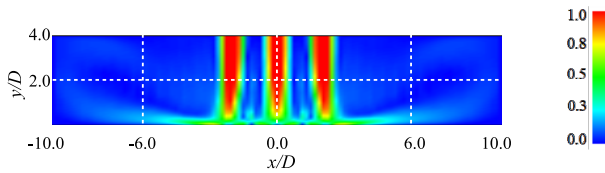


Figure 7: Contour of mean velocity magnitude on plane1 (7 jets)

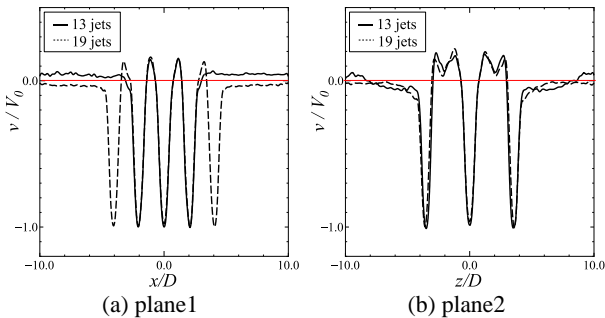
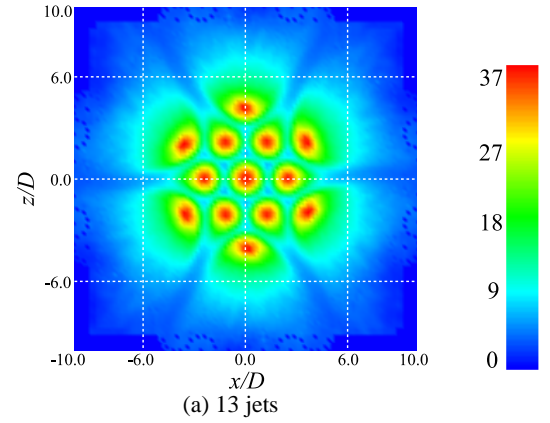
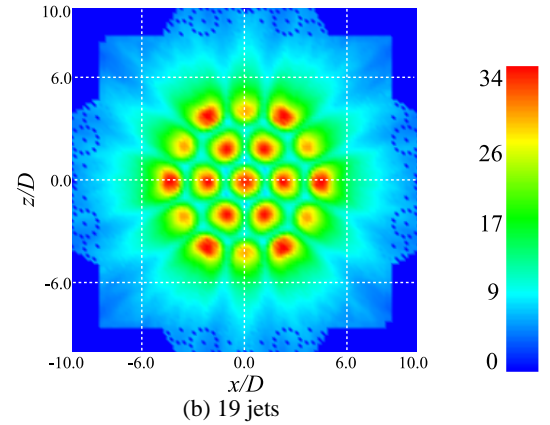


Figure 8: Distribution of normal velocity

each jet issues, impinges and then spreads over the impingement wall. The flow over the impingement wall blows out strongly between the outer jets. The contours of time-averaged velocity magnitude on the  $x-y$  plane (plane1) and  $y-z$  plane (plane2) through the central jet located at  $x = z = 0$  are shown in figure 5 and 6, respectively. The high-speed region indicated by red color corresponds to free jet region categorized in [7, 14]. According to the cutting plane, i.e., plane1 and 2, the existence of three or five jets are confirmed. The velocity magnitude of each jet is reduced as approaching the impingement wall, in addition, the central jet seems to be a nearly axisymmetric, while the outer jets are not. This characteristics are qualitatively the same in both plane1 and 2. The characteristics of flow regions indicated by green in the vicinity of the impingement wall show different features between plane1 and 2. In case of the 13 jets,



(a) 13 jets



(b) 19 jets

Figure 9: Contour of mean local Nusselt number

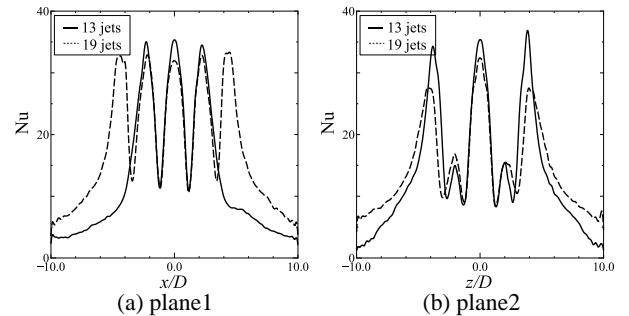


Figure 10: Distribution of mean local Nusselt number

on plane1, the flow region spreads away from the impinging surface and then, a radially outer flow (cross flow) appears. On the other hand, on plane2 the wall jet spreads along the wall. In case of the 19 jets, a wall jet is generated on plane1, and a cross flow occurs on plane2. In order to investigate the reason why the cross flow occurs, a case with 7 jets obtained by removing 6 outer jets from the 13 jets is examined. In figure 7, it can be seen that cross flow is not confirmed, and that the flow in the vicinity of the impingement wall, i.e., wall jet is formed. Thus, it turns out that the equipment of outer jets determines the occurrence of a cross flow, while since in the 19 jets the cross flow is not observed, thus increasing number of outer jet does not always contribute to the cross flow formation. In order to quantitatively investigate the flow feature between the jets, figure 8 shows the wall-normal velocity distribution at  $y/D = 2.0$  on plane1 and 2. It can be seen that the up-wash flow ( $v > 0$ ) is generated in the direction opposite to the issuing flow

from the inlet. There is no obvious difference in the value of the up-wash peak between plane1 and 2. But in the direction parallel to the horizontal axis, the scale of the up-wash flow on plane2 is larger than that on plane1. The large-scale up-wash structure is formed between jets on plane2. The 13 and 19 jets have the same characteristics in the points that the up-wash flow is generated.

#### Heat transfer characteristics

In order to evaluate the qualitative heat transfer characteristics of the time-averaged local Nusselt number contour on the impingement wall is shown in figure 9.  $Nu$  is defined with  $Nu = \frac{\partial T}{\partial y} \Big|_{y=0} \frac{D}{T_o - T_w}$ . In general, it is well known that SIJ has high heat transfer performance in the stagnation region formed in the vicinity of the impingement point; the heat transfer performance decreases radially as the radial distance increases [7, 14]. From figure 9, the characteristics of SIJ remain even in the MIJ; high heat transfer performance near the impinging point of each jet and the heat transfer performance promptly decays away from jet itself. The heat transfer performance between the impinging jets decreases by the influence of interference as mentioned in previous literatures [13, 15]. In addition, high heat transfer area of the central jet distributes as a circle, but that of the outer jet is elliptical. Such a feature is attribute to the modulation of impinging flow as mentioned in figure 5. Focusing on the outer jet of the 19 jets, the Nusselt number of the outer jets alternately varies along azimuthal direction. Namely, compared the 13 and 19 jets, even though 6 jets are added to outer of the 13 jets, the distribution of peak value is influenced, peculiar pattern in the 19 jets appears. It demonstrates that the local heat transfer performance of MIJ is not well predictable using that of similar MIJ. In order to quantitatively evaluate the local heat transfer characteristics, the distribution of Nusselt number on plane1 and 2 are shown in figure 10. As can be confirmed in figure 9, the peak of Nusselt number is formed at the impingement point and decreases towards the outside. At the same time, the peak value of the 19 jets is lower than the 13 jets, however, since the strength of cross flow directly depends on the number of jet, the cross flow of the 19 jets induces high forced convection, resulting in higher heat transfer outside of MIJ. Although the heat transfer performance between the jets is reduced by interference, a different distribution of Nusselt numbers between plane1 and 2 appears: only one minimum between jets is on plane1, a peak and two valley on plane2. The peak value of Nusselt number between jets on plane2 is taken by the combination of adjacent jet flow interference. Not shown here, we confirm the valley corresponds to a center enclosed by the three jets.

#### Conclusions

In the present study, in order to elucidate the flow and heat characteristics of multiple impinging jets, we conduct the DNS of 13 and 19 round impinging jets. Conclusions are as follows:

- In MIJ, it reveals that the formation of up-wash flow between jets and of cross flow is attributed to the jet-jet interaction, and that the combination of these flow induces complex flow field of MIJ.
- From analysis of the heat transfer performances, the peaks of Nusselt number are formed around impinging position of each jet, demonstrating even in the MIJ non-uniform distribution are formed. Although the cross flow slightly reduces the local peaks of Nusselt number, however, heat transfer surroundings of MIJ is enhanced due to the cross flow.

#### References

- [1] Aldabbagha, L.B.Y. and Mohamad, A.A., A three-dimensional numerical simulation of impinging jet arrays on a moving plate, *Int. J. Heat and Mass Transfer*, Vol.52 (2009), pp.4894-4900.
- [2] Canuto, C., Hussaini, M.Y., Quarteroni, A.M., Zang, Th.A., J, *Spectral Methods in Fluid Dynamics*, 1993
- [3] Draksler, M., Ničeno, B., Končar, B., and Cizelj, L., Large eddy simulation of multiple impinging jets in hexagonal configuration - mean flow characteristics, *Int. J. Heat and Fluid Flow*, Vol. 46 (2014), pp.147-157.
- [4] Geers, L.F. G., Hanjalić, K., and Tummers, M. J. D., Wall imprint of turbulent structures and heat transfer in multiple impinging jet arrays, *J. Fluid Mech.*, Vol. 546 (2006), pp.255-284.
- [5] Hadžabdžić, M. and Hanjalić, K., Vortical structures and heat transfer in a round impinging jet, *J. Fluid Mech.*, Vol. 596 (2007), pp.221-260.
- [6] Hattori, H. and Nagano, Y., Direct numerical simulation of turbulent heat transfer in plane impinging jet, *Int. J. Heat and Fluid Flow*, Vol. 25 (2004), pp.749-758.
- [7] Kataoka, K., Impingement heat transfer augmentation due to large scale eddies, *In Heat Transfer 1990, Proc. 9th Intl Heat Transfer Conf.*, Vol. 1 (1990), pp.255-273.
- [8] Lele, S. K., Compact finite difference schemes with spectral-like resolution, *J. Comp. Phys.*, Vol.103 (1992), pp.16-42.
- [9] Martin D. et al. , Large Eddy Simulation of multiple impinging jets in hexagonal configuration - Flow dynamics and heat transfer characteristics , *Int. J. of Heat and Mass Trans.*, Vol 109 (2017), pp.16-27.
- [10] Nordstrom, J., Nordin, N., and Henningson, D. S., The fringe region technique and the fourier method used in the direct numerical simulation of spatially evolving viscous flows, *SIAM J. Sci. Comp.*, Vol. 20, No.4 (1999), pp.1365-1393.
- [11] Silva, C. B. and Metais, O., Vortex control of bifurcating jets: A numerical study, *Phys. Fluids*, Vol.14(2002), pp.3798-3819.
- [12] Tsubokura, M., T.Kobayashi, T., Taniguchi, N. and Jones, W. P., A numerical study on the eddy structure of impinging jets excited at the inlet, *Int.J. Heat and Fluid Flow*, Vol. 24(2003), pp.500-511.
- [13] Tsujimoto, K., Kariya, S., Shakouchi, T. and Ando, T., Investigation on Jet Mixing Rate Based on DNS of Excitation Jets, *Trans. JSME* , Vol.74, No.737B(2008), pp.34-41.(in Japanese)
- [14] Viskanta,R., Heat transfer to impinging isothermal gas and flame jets, *Exp. Therm. Fluid Sci.*, Vol. 6(1993), pp.111-134.
- [15] Weigand, B. and Spring, S., Multiple jet impingement - a review, *Heat Transfer Res.*, Vol. 42, No.2(2011), pp.101-142.